

Phase ordering and shape deformation of two-phase membranes

Y. Jiang[†], T. Lookman^{*}, and A. Saxena

Theoretical Division, Los Alamos National Laboratory, Los Alamos, New Mexico 87545

**Department of Applied Mathematics, University of Western Ontario, London, Ontario, N6A 5B7 Canada*

Within a coupled-field Ginzburg-Landau model we study analytically phase separation and accompanying shape deformation on a two-phase elastic membrane in simple geometries such as cylinders, spheres and tori. Using an exact periodic domain wall solution we solve for the shape and phase ordering field, and estimate the degree of deformation of the membrane. The results are pertinent to a preferential phase separation in regions of differing curvature on a variety of vesicles.

Amphiphilic molecules assemble in aqueous media to form bilayers, which close to form vesicles at low concentrations. Bilayers and vesicles serve as models for membranes and cells for studying simple physical properties such as shape deformations, elasticity and transport. They show an amazing variety of shapes, which have been described by treating the membrane as a homogeneous elastic sheet with area and volume constraints [1,2]. However, recent experimental observations have recognized that internal degrees of freedom can crucially influence the shapes. An example is the transition from a normal biconcave shape of *discocytes* to a crenated shape of *echinocytes* of a human red blood cell. Such transformations can be induced by an asymmetric adsorption of certain drugs, i.e., a local asymmetry in the composition plays an important role in this crenated shape [3].

As molecules are free to move in the plane of the membrane, lateral phase separation is constantly observed in lipid membranes. A single component membrane under certain conditions can exhibit regions rich in tilted and non-tilted phases, respectively, while a two-component membrane can exhibit phase separation of both different components and tilted vs. non-tilted phases [4]. Phase separation plays a central role in the stabilization of vesicles and in the fission of small vesicles after budding [5,6]. Although experimental studies that clearly relate phase separation to local shape deformation [4] are scarce, a number of phenomenological and numerical investigations have shown that a coupling of the local curvature to the local composition of amphiphiles can result in shape deformation [7–9] and budding [10].

The numerical studies have considered mainly a general fluctuating vesicle and therefore the central role of the coupling between the phase separation and accompanying shape deformation process has been difficult to decipher. Our work is thus motivated by a desire to study, by analytical means where possible, phase separation on the simplest of geometries such as cylinders, spheres and

tori. While microtubules are abundant in biology, deformable spherical and toroidal vesicles have also been observed [11]. We seek to provide a systematic formal description of the equilibrium solution. Our aim is to gain insight into the part played by curvature and to extract the salient ingredients that affect phase separation and shape changes. We estimate the degree of deformation from the coupling strength between the composition and curvature fields and the elastic rigidity.

We represent a membrane as a surface embedded in three dimensions parameterized by $q \equiv \{q_1, q_2\}$, for its thickness is usually several orders of magnitude smaller than its size. Our approach is to study phase separation on a subset of surfaces (orthogonal curvilinear manifolds [12]) which have either an axis of translation or rotation. For this special class of surfaces we have recently derived some simplifying analytical results regarding phase separation on *rigid* curved surfaces [13]. Here we apply the analysis to deformable surfaces.

The total free energy of the membrane is $F = F_1 + F_2 + F_3$, with the bending elastic energy [2]:

$$F_1 = \int dA \left[\frac{\kappa}{2} (h - h_0)^2 \right], \quad (1)$$

where $dA = \sqrt{g} d^2q$ is the area element with \sqrt{g} the determinant of the metric tensor g_{ij} , h the mean curvature, and h_0 the spontaneous mean curvature—the preferred curvature of the relaxed vesicle. The mean curvature is $h = h(q_1, q_2) = h_1 + h_2$, where h_1 and h_2 are the principal curvatures. For an arbitrary surface embedded in three dimensions, if q_1 and q_2 are orthogonal coordinates, the metric tensor has $g_{ij} = 0$ for $i \neq j$ and $\sqrt{g} = \sqrt{g_{11}g_{22}}$.

We treat phase separation within the usual Ginzburg-Landau free energy framework:

$$F_2 = \int dA \left[\frac{\xi^2}{2} |\nabla \phi|^2 + V(\phi) \right], \quad (2)$$

where ϕ is either the relative concentration of the two phase components A and B of the membrane: $\phi = (A - B)/(A + B)$, or the concentration of a diffusing external chemical, as in the case of *echinocytosis* of red blood cells [3,14]. Here ξ is the characteristic length, which determines interface width.

We use the bilinear form of coupling between the phase density and local curvature [14], an interaction energy found on phenomenological grounds:

$$F_3 = \int dA \Lambda \phi h, \quad (3)$$

where Λ is the strength of the coupling.

More realistic considerations should take into account area and volume constraints for vesicle membranes. A change in area would increase the surface energy and a change in volume would increase the osmotic pressure. Hence an additional term

$$F_4 = \lambda A + PV = \int dA (\lambda + P \frac{|r|}{3}), \quad (4)$$

where λ is the surface tension and P the osmotic pressure, should be included in the free energy F . The second term in the expression utilizes the divergence theorem in 3D. The surface tension λ is a constant and does not enter the variational calculations. The relation between the local radius $|r|$ and the mean curvature h can be highly complicated depending on the geometry, which will render the free energy too intractable for our purposes. Therefore, we consider only $P = 0$ hereafter.

In the case where the order parameter is conserved, as we consider no exchange of molecules of the membrane with its environment, an appropriate equation for the time evolution of the phase ordering field ϕ is:

$$\frac{\partial \phi}{\partial t} = \Gamma_1 \nabla_{LB}^2 \frac{\delta F}{\delta \phi} = \Gamma_1 \nabla_{LB}^2 [V'(\phi) - \nabla_{LB}^2 \phi + \Lambda h],$$

where prime denotes differentiation with respect to ϕ . Similarly, for the mean curvature:

$$\frac{\partial h}{\partial t} = \Gamma_2 \nabla_{LB}^2 \frac{\delta F}{\delta h} = \Gamma_2 \nabla_{LB}^2 [(\kappa(h - h_0) + \Lambda \phi)],$$

where Γ_1 and Γ_2 are the diffusion coefficients for ϕ and h fields, respectively, and $\nabla_{LB}^2 \equiv \frac{1}{\sqrt{g}} \frac{\partial}{\partial x^i} (g^{ij} \sqrt{g} \frac{\partial}{\partial x^j})$ is the Laplace-Beltrami operator. As the details of the double-well potential are not important [15], we use a simple ϕ^4 potential to describe the phase separation dynamics: $V(\phi) = \frac{\alpha}{4} \phi^4 - \frac{\beta}{2} \phi^2$, ($\alpha, \beta > 0$).

The numerical study of the dynamics of evolution will be reported elsewhere [16]. Here we focus on the analytic equilibrium solutions. At equilibrium, the Euler-Lagrange (EL) equations for ϕ and h fields are $\delta F / \delta \phi = 0$ and $\delta F / \delta h = 0$, respectively. The EL equations are nonlinear and usually do not have an exact closed-form solution. In order to obtain analytical results, we consider special symmetries to reduce the problem to a quasi-one dimensional one. If q_1 is the axis of symmetry, $|\nabla \phi| = |d\phi/dq_2|$. We then define a new variable τ_1 as $d\tau_1 \equiv \sqrt{g_{22}/g_{11}} dq_2$. With this new variable, $\nabla_{LB}^2 \phi = \frac{1}{g_{11}} \frac{d^2}{d\tau_1^2} \phi$.

The equilibrium condition, derived from the EL equation for h is

$$h = h_0 - \frac{\Lambda}{\kappa} \phi, \quad (5)$$

i.e., at equilibrium the local mean curvature of the membrane is linearly proportional to the local ϕ . This linear relationship explains why phase separated regions have

local curvature $(\Lambda/\kappa)\phi$, a result that appeared in the numerical study of Ref. [9]. Thus, we can eliminate h from the free energy. It follows that the EL equation for the free energy with respect to ϕ becomes

$$V'_e(\phi) - \frac{d^2}{d\tau_1^2} \phi = 0. \quad (6)$$

Here V_e is the new effective potential:

$$V_e \equiv g_{11} \left[\frac{\alpha}{4} \phi^4 - \frac{1}{2} (\beta + \frac{\Lambda^2}{\kappa}) \phi^2 + \Lambda h_0 \phi \right], \quad (7)$$

which depends only on ϕ . The coefficient of the ϕ^2 term is renormalized and the effective potential becomes an asymmetric double-well due to the linear coupling.

Twice integrating Eq. (6) we obtain a general periodic domain-wall lattice solution:

$$\phi(\tau) = d + \frac{c - d}{1 - \frac{b-c}{b-d} \text{sn}^2\left(\frac{\tau - \tau_0}{\zeta}, k\right)}, k \equiv \sqrt{\frac{(b-c)(a-d)}{(a-c)(b-d)}}, \quad (8)$$

where $d\tau \equiv d\tau_1 \sqrt{g_{11}} = \sqrt{g_{22}} dq_2$ is the arc length variable; a, b, c and d are real roots of $V_e - V_0 = 0$, i.e. $V_e - V_0 = g_{11}(\phi - a)(\phi - b)(\phi - c)(\phi - d)$ with $a > b \geq \phi > c > d$; V_0, τ_0 are two constants of integration, $\zeta \equiv \xi \sqrt{4/\alpha} \sqrt{2/(a-c)(b-d)}$ is the rescaled characteristic length scale, k is the modulus of the Jacobian elliptic function $\text{sn}(\tau, k)$. The shape of the periodic solution depends on the modulus k , which in turn depends on all the parameters of the model and the boundary condition V_0 . The value of k ranges between 0 and 1. For $k = 0$, the Jacobian elliptic function reduces to a sinusoidal function. For $k = 1$, $\text{sn}(\tau, k)$ changes to a kink solution, $\tanh(\tau)$, which is no longer periodic and thus is only allowed on an open geometry. For a closed geometry, e.g. a circle, a periodic solution is required and the number of periods for a fixed perimeter L depends on the value of k [17]: the periods allowed should satisfy $L/\zeta = 4mK$ where $K(k)$ is the complete elliptic integral of the first kind and m is an arbitrary integer. With the linear relationship between ϕ and h , Eq. (5), we also obtain the expression for the mean curvature $h(\tau) = h_0 - \frac{\Lambda}{\kappa} \phi(\tau)$.

Transforming τ to space coordinate q_2 and exploiting the fact that q_1 is the axis of symmetry, we obtain $\phi(q_1, q_2)$ and $h(q_1, q_2)$. From $h(q_1, q_2)$, we can then use the relationship between h and r , to obtain $r(q_1, q_2)$, the shape in real space coordinates.

For illustration purposes, we now carry out this formulation on a cylinder with rotational symmetry $r = r(z)$. The metric tensor has $g_{\theta\theta} = r^2$, $g_{zz} = 1 + r'^2$ and $g_{\theta z} = 0$.

With θ as the axis of symmetry, we define the new variable τ_1 as

$$d\tau_1 = dz \sqrt{\frac{g_{zz}}{g_{\theta\theta}}} = dz \sqrt{\frac{r^2 + r'^2}{r^2}}.$$

The free energy for such a cylinder is then

$$F = \int d\tau_1 d\theta \left[\frac{\xi^2}{2} \phi_{\tau_1}^2 + V_e(\phi) \right], \quad (9)$$

in which $V_e(\phi)$ is the same as Eq. (7). Applying the EL equation for h , we obtain the same linear relation between h and ϕ as in Eq. (5) in terms of τ_1 . Replacing h in the free energy, F becomes a function of ϕ only and its EL equation with respect to ϕ is

$$\frac{\delta F}{\delta \phi(\tau_1)} = \xi^2 \phi_{\tau_1 \tau_1} - r^2 \left[\alpha \phi^3 - \left(\beta + \frac{\Lambda^2}{\kappa} \right) \phi + \Lambda h_0 \right] = 0.$$

This equation yields the same solution for ϕ as Eq. (8) as a function of the arc variable τ :

$$d\tau \equiv r d\tau_1 = dz \sqrt{1 + r'^2}, \quad (10)$$

and hence the solution of $h(\tau)$ based on the linear relationship between ϕ and h .

In order to convert the ϕ and h results to phase distribution and deformation on a cylinder, i.e., to obtain $\phi(z, \theta)$ and $r(z, \theta)$, we need to change the variable τ back to the original variable z as follows. We replace $r = r(z)$ by $\rho(\tau)$, such that

$$\rho_\tau = r_z / \sqrt{1 + r_z^2}, \quad \rho_{\tau\tau} = r_{zz} / (1 + r_z^2).$$

The mean curvature $h(z)$ in terms of $\rho(\tau)$ is

$$h(\tau) = 1/\rho + \rho_{\tau\tau} / \sqrt{1 - \rho_\tau^2}. \quad (11)$$

A numerical integration of this equation provides $\rho(\tau)$ and thus $z = \int d\tau \sqrt{1 - \rho_\tau^2}$, which in turn gives $r(z) = \rho(\tau(z))$, the deformation along the z axis of a cylinder.

Figure 1a shows a typical plot for the equilibrium ϕ , h and r as a function of z , obtained with the following parameters: $\alpha = 4$, $\beta = 2$, $h_0 = 5$, $\xi = 0.2$, $\kappa = 0.02$, and $\Lambda = 0.03$. Figure 1b is the corresponding *axially* deformed cylinder, whose shades of gray correspond to the amplitude of the order-parameter field. Applying the same formulation to a cylinder with an axial symmetry $r = r(\theta)$, we obtain a cylinder with deformation occurring only along the cross section. Figure 2a shows a series of deformed circles with periods 3 to 6. A *radially* deformed cylinder, as shown in Fig. 2b, is formed by translating the deformed circle along the z axis. Figure 2b uses the same parameters as in Fig. 1.

The degree of deformation, defined as the ratio of the maximum to the minimum radii, $D = r_{\max}/r_{\min}$, is a quantity that can be measured by reflection interference contrast microscopy [18] or atomic force microscopy [19]. We estimate the degree of deformation of an axially symmetric cylinder, for which $r = 1/H$ and thus $D = (H_0 - \frac{\Lambda}{\kappa}c)/(H_0 - \frac{\Lambda}{\kappa}d)$, as a function of κ and Λ . The value of κ can be either obtained by using micropipette methods [20], or estimated from molecular

dynamics simulations [21]. Although difficult to measure directly in experiments, Λ may be derived from first principle molecular dynamics simulations as in [21] by using Eq. (5). Figure 3a shows that the deformation D has a quadratic form in $1/\kappa$. Figure 3b indicates again a quadratic form dependence of the deformation on the coupling constant Λ . This can be understood by expanding D in the small deformation limit, when $\Lambda \ll \kappa$. In this limit, $c - d$ and cd remain approximately independent of Λ and κ , thus $D \propto c_1 + c_2\Lambda/\kappa + c_3\Lambda^2/\kappa^2$ with c_1, c_2 and c_3 constants. Indeed, if we vary both Λ and κ such that Λ/κ remains constant, the deformed circles are virtually identical (figure not shown).

We also applied this framework to other deformable geometries and symmetries, e.g. a sphere and a torus with appropriate g_{ij} . Figures 4a,b and 4c,d show results for spheres and tori with axial and azimuthal symmetry, respectively. The parameters used are the same as in Fig. 1. We observe preferential phase separation similar to the case of cylinders.

To summarize, we have developed a theoretical framework in which we obtained exact analytical solutions for the equilibrium phase distributions and membrane shapes, for a series of geometries including cylinders, spheres and tori. This framework allows for an estimate of the degree of deformation from the coupling strength and the elastic rigidity of the membrane. Since fluid properties are essential for modeling cells and membranes, our model augmented with a coupling to hydrodynamics will enable the study of realistic biological cells.

The order-parameter field considered above need not be a scalar density or relative concentration field. If we choose magnetization (M) or polarization (P) instead of ϕ , we would then expect periodic stripes of magnetic and polarization domains in regions of different curvature.

We thank R.C. Desai and G. L. Eyink for useful discussions. This research is supported in part by the US Department of Energy, under contract W-7405-ENG-36.

[†] Electronic address: jiang@lanl.gov.

- [1] P. B. Canham, J. Theor. Biol. **26**, 61 (1970).
- [2] W. Helfrich, Z. Naturforsch **28c**, 693 (1973). H. J. Deuling and W. Helfrich, Biophys. J. **16**, 861 (1976).
- [3] M. P. Sheetz, et al., J. Cell Biol. **70**, 193 (1976).
- [4] G. Gebhardt, H. Gruler, and E. Sackmann, Z. Naturforsch. **32C**, 581 (1977).
- [5] F. Jülicher and R. Lipowsky, Phys. Rev. Lett. **70**, 2964 (1993).
- [6] H.-G. Döbereiner *et al.*, Biophys. J. **65**, 1396 (1993).
- [7] E. Sackmann and T. Feder, Mol. Membrane Biol. **12**, 21 (1995).
- [8] T. Kawakatsu et al., J. Phys. II (France) **3**, 971 (1993); T. Taniguchi et al., *ibid.* **4**, 1333 (1994).

- [9] T. Taniguchi, Phys. Rev. Lett. **76**, 4444 (1996).
- [10] P. B. S. Kumar and M. Rao, Phys. Rev. Lett. **80**, 2489, (1998).
- [11] X. Michalet and D. Bensimon, Science **269**, 666 (1995).
- [12] See e.g. G. Arfken, *Mathematical Methods for Physicists*, (Academic, New York, 1970), 2nd edition, Chapt. 2.
- [13] A. Saxena and T. Lookman, Physica D **132**, (1999).
- [14] S. Leibler, J. Phys. **47**, 507 (1986).
- [15] A. J. Bray, Adv. Phys. **43**, 357 (1994).
- [16] Y. Jiang, T. Lookman, and A. Saxena, in preparation.
- [17] See e.g. M. Dinter, Phys. Rev. B **39**, 8423 (1989); P. Byrd, M. Friedman *Handbook of Elliptic Integrals for Engineers and Physicists*, (Springer, Berlin 1971), 2nd ed.
- [18] E. Sackmann, FEBS Lett. **346**, 3 (1994).
- [19] B. D. Ermi, A. Karim, and J. F. Gouglas, J. Polymer Sci. **36 B**, 191 (1998).
- [20] E. Evans and W. Rawicz, Phys. Rev. Lett. **79**, 2379 (1997).
- [21] R. Goetz, G. Gompper, and T. Lipowsky, Phys. Rev. Lett. **82**, 221 (1999).

FIG. 1. Phase separation and deformation on a radially symmetric circular cylinder. (a) Plots of order parameter ϕ , curvature h and radius r as a function of z . (b) Equilibrium shape of the deformed cylinder; shades of gray correspond to the order-parameter ϕ .

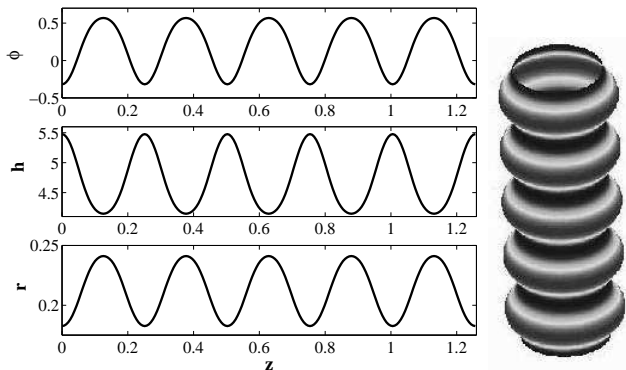


FIG. 2. Phase separation and deformation on an axially symmetric circular cylinder. (a) Cross sections of deformed cylinder with 3, 4, 5 and 6 modes, respectively. (b) Equilibrium shape of a deformed cylinder with mode 6; shades of gray correspond to the order parameter ϕ .

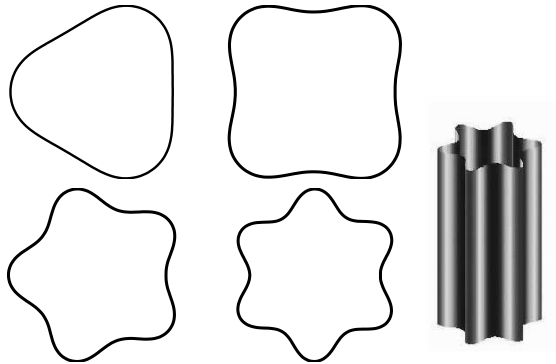


FIG. 3. Deformation of the axially symmetric cylinder as a function of: (a) Elastic rigidity κ for fixed $\Lambda = 0.02$; circles are numerical data and the solid line is fit Inset shows the deformed cross sections of the cylinder, the inner-most curve corresponding to smallest κ value. (b) Coupling constant Λ for fixed $\kappa = 0.01$; circles are numerical data and the solid line is a fit to a quadratic form. Inset shows the deformed cross sections with fixed perimeter, the inner-most curve corresponds to the largest Λ value.

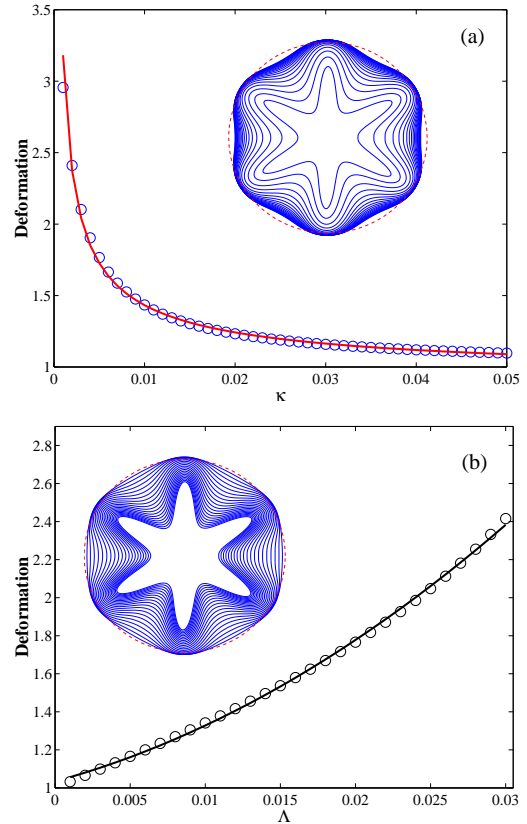


FIG. 4. Phase separation and deformation on spheres and tori. (a) Axially symmetric sphere. (b) Azimuthally symmetric sphere. (c) Axially symmetric torus. (d) Azimuthally symmetric torus. Shades of gray correspond to different magnitudes of the order parameter ϕ .

